

Design, Analysis and Experimental Modal Testing of a Mission Adaptive Wing of an Unmanned Aerial Vehicle

Melin Şahin*, Yavuz Yaman, Serkan Özgen, Güçlü Seber
Aerospace Engineering, Middle East Technical University,
*melin@ae.metu.edu.tr
İnönü Bulvarı, 06531, Ankara, Turkey

Evren Sakarya†, Levent Ünlüsoy, E. Tolga İnsuyu
Aerospace Engineering, Middle East Technical University,
†esakarya@ae.metu.edu.tr
İnönü Bulvarı, 06531, Ankara, Turkey

Abstract - The mission adaptive wings aim to overcome the inefficient behaviour of the classical fixed wings, especially for the off-design conditions, by changing their geometry actively to adopt to changing flight conditions for maximized performance. This study presents the structural design, analysis and experimental modal testing of an unmanned aerial vehicle wing having mission adaptive characteristics.

I. INTRODUCTION

The mission adaptive components of the aerial vehicles have the capability to change their shape in order to adapt themselves to the changing flight conditions and/or the mission profile of the vehicle. The aims of the flight vehicles having mission adaptive components are to fly different kinds of missions, perform effective manoeuvres and have increased fuel efficiency [1]. In general, this can be managed via concepts creating various morphing features in the wings. This study presents the structural design, analysis and experimental modal testing of an unmanned aerial vehicle wing having mission adaptive characteristics.

II. STRUCTURAL DESIGN OF MISSION ADAPTIVE WING

The structural modelling of the designed wing [2] was conducted by using the Finite Element Method and MSC® PATRAN Package program [3]. The wing structure was mainly composed of four substructures; which were spars, webs, skin and connectors. Spar webs were modelled by using 2D shell element in order to get torsion response where the spar flanges were modelled using 1D beam elements to get more accurate results in bending responses. Skins and webs were also modelled using 2D shell elements. Finite element models of spar and rib structures are shown in Fig. 1 and 2 respectively. The geometric model of the wing inner structure is shown in Fig. 3 and the outer view of the wing torque-box is given in Fig. 4.

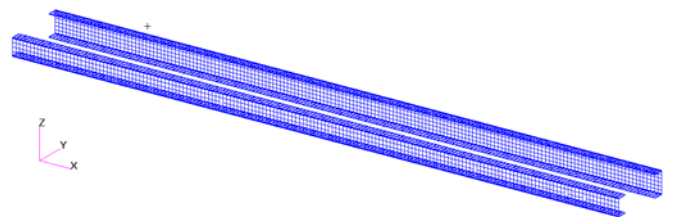


Fig. 1. Finite element model of the spar webs

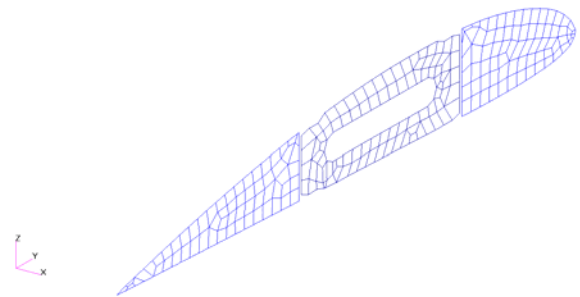


Fig. 2. Finite element model of a typical rib

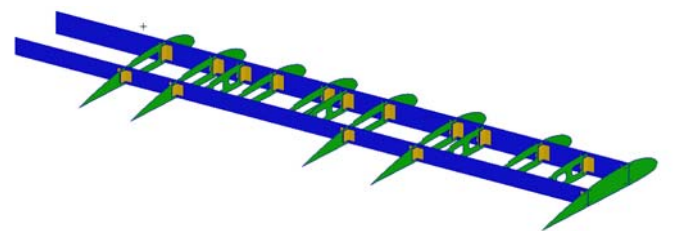


Fig. 3. Geometric model of the wing inner structure

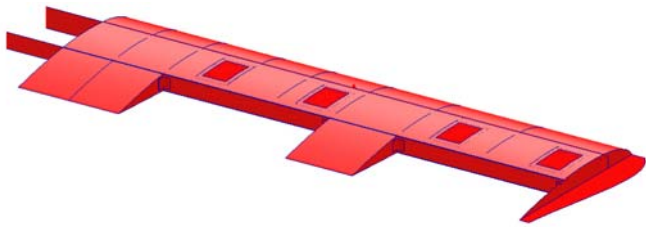


Fig. 4. Geometric model of the wing torque-box

The mission adaptive components of the wing are the hingeless control surfaces [4] with open trailing edges which were modelled in MSC[®] PATRAN. The characteristics of the inner components of the control surfaces were determined by using the nonlinear analysis module in MSC[®] NASTRAN. Finite element model of a typical hingeless control surface is shown in Fig 5 [5].

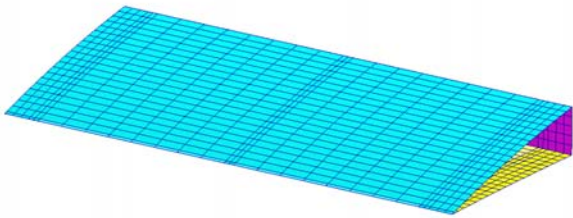


Fig. 5. Finite element model of a typical hingeless control surface

After the manufacturing and before the implementation on the wing; the hingeless control surfaces were tested with various servo control surfaces. Fig. 6 shows the hingeless control surface in constant positive chord-wise actuation and Fig. 7 gives the view of constant negative chord-wise actuation. The twisting loads were also applied to the hingeless control surface. The twisting actuation of the hingeless control surface is shown in Fig. 8. In Fig. 9 and Fig. 10, the geometric model of the mission adaptive wing and its finite element model are presented respectively.



Fig. 6. Hingeless control surface with constant positive chord-wise actuation



Fig. 7. Hingeless control surface with constant negative chord-wise actuation



Fig. 8. Hingeless control surface with twisting actuation

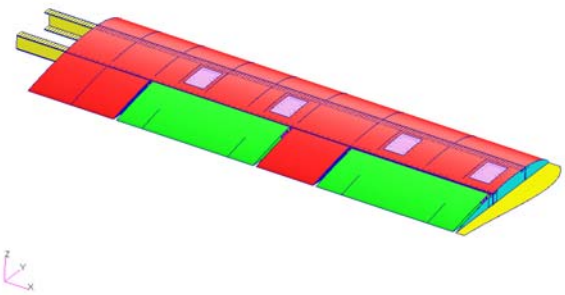


Fig. 9. Geometric model of the mission adaptive wing

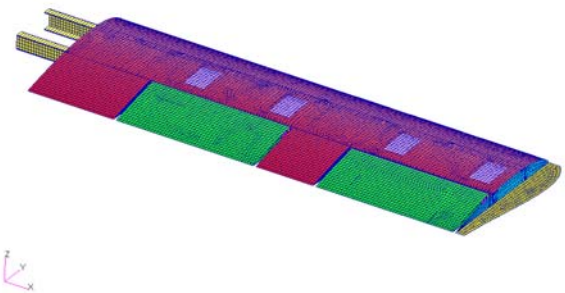


Fig. 10. Finite element model of the mission adaptive wing

III. MODAL ANALYSIS OF MISSION ADAPTIVE WING

Modal analysis of the mission adaptive wing was done with Normal Mode Analysis (Solution 103) of MSC® NASTRAN. Global bending and torsion modes of the mission adaptive wing and corresponding natural frequencies are presented in Table I.

TABLE I
NATURAL FREQUENCIES AND THE ASSOCIATED MODES
(FINITE ELEMENT ANALYSIS)

Mode Shape	Natural Frequency [Hz]
1 st Out-of-plane Bending	13.52
1 st Torsion	46.30
2 nd Out-of-plane Bending	87.69

The first out-of-plane bending mode, the first torsional mode and the second out-of-plane bending mode of the wing are shown in Fig. 11, Fig. 12. and Fig. 13, respectively. In these figures, hingeless control surfaces and tip fairing are not shown in order to better visualize the global modes of the wing as aforementioned components have high eigenvectors compared to other parts of the wing.

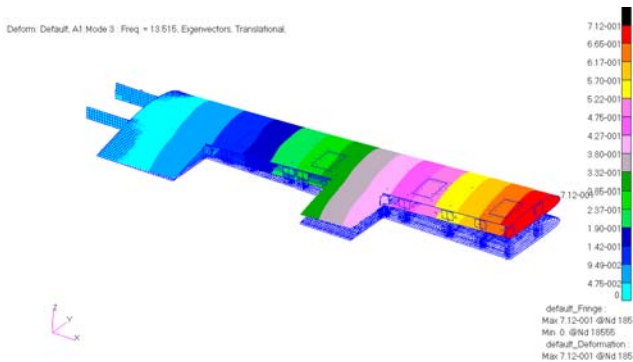


Fig. 11. 1st out-of-plane mode shape of the mission adaptive wing (f= 13.52 [Hz])

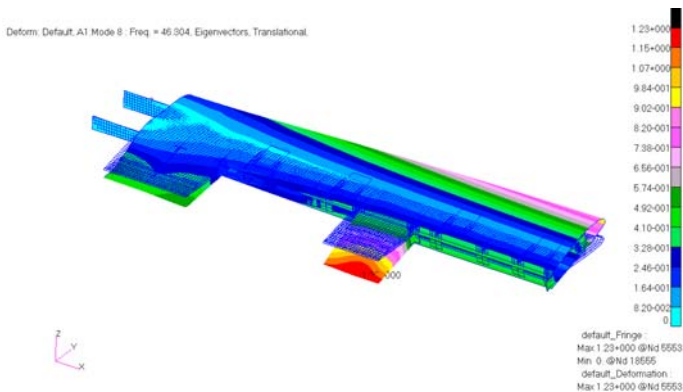


Fig. 12. 1st torsional mode shape of the mission adaptive wing (f= 46.30 [Hz])

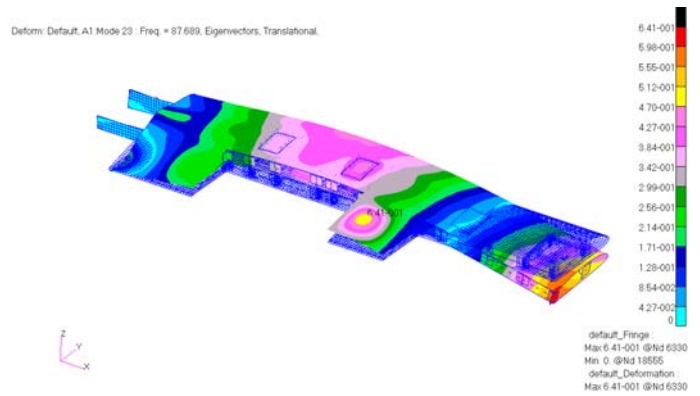


Fig. 13. 2nd out-of-plane mode shape of the mission adaptive wing (f= 87.69 [Hz])

IV. EXPERIMENTAL MODAL TESTS OF MISSION ADAPTIVE WING

Experimental setup used during the experimental modal analysis is shown in Fig. 14 and the mission adaptive wing attached to fixture with modal shaker is shown in Fig. 15. B&K 4508B single axis accelerometers [6] were used to measure the acceleration of the wing and B&K 4825 modal shaker [7] and B&K 8206 impact hammer [8] were used to excite the wing.



Fig. 14. Equipment used in the experimental modal analysis



Fig. 15. The mission adaptive wing, modal shaker and accelerometers in the experimental modal analysis

Fig. 16 shows the wing torque box geometry definition for the experiments. Nodes 64-67 were used to define the boundary conditions and nodes 1-63 were used as the excitation points of roving impact hammer. The stationary single axis accelerometers were placed in nodes 10, 29 and 54 in order to get the comparative data. Modal shaker was acted at node 5. Measurements on the control surfaces were done by accelerometers placed on each of them; no excitation was applied on the control surfaces.

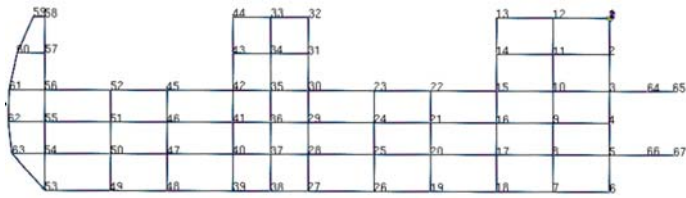


Fig. 16. Experimental grid of the wing torque-box

The following procedure was employed during the experiments. First the wing was excited by the impact hammer to locate the ranges of the resonances. The wing was then excited by using a modal shaker and white noise type excitation. This gives the accurate locations of the resonant frequencies. The wing was finally excited by using the modal shaker but this time with a sine sweep signal. That helps to verify the accurate resonant frequencies.

A typical frequency response function, which was between accelerometer in node 54 and white noise excitation from node 5 by the modal shaker, is presented in Fig. 17. Frequency response functions obtained in hammer tests from three accelerometers, each of which having 63 measurements are shown in Fig. 18 and their average is given in Fig. 19.

The mode-shape at the resonance frequencies were determined by using roving-hammer test. The mode shapes associated with the resonant frequencies found were plotted by the use of imaginary part of the frequency response data and global modes were identified. Mode shapes for out-of-plane bending modes and torsional modes are presented in Fig. 20 to Fig. 22. In the figures, the horizontal axes are in cm and the vertical axis is normalized for visualization.

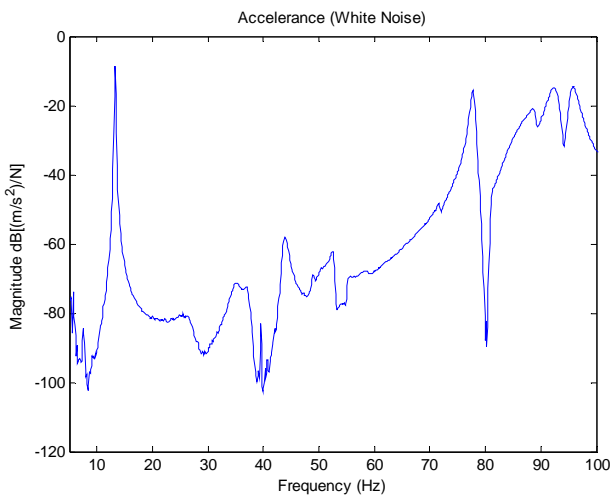


Fig. 17. Frequency response function between accelerometer in node 54 and white noise excitation given at node 5

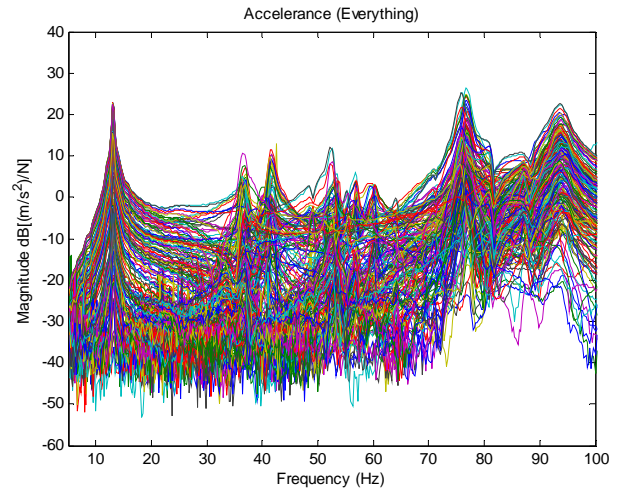


Fig. 18. Frequency response functions of the roving hammer measurements

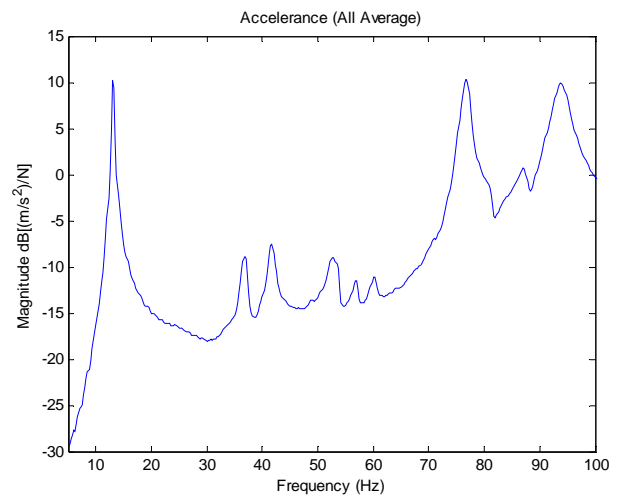


Fig. 19. Average frequency response function of the roving hammer measurements

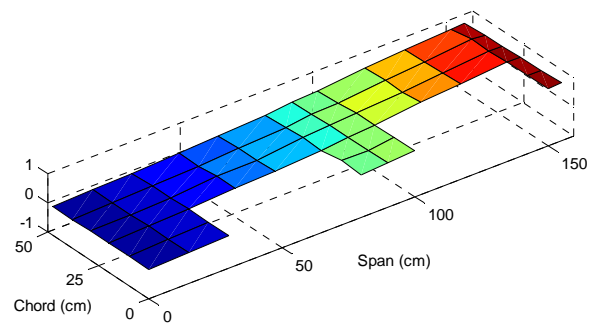


Fig. 20. Experimental 1st out-of-plane mode shape of the mission adaptive wing ($f=13.00$ [Hz])

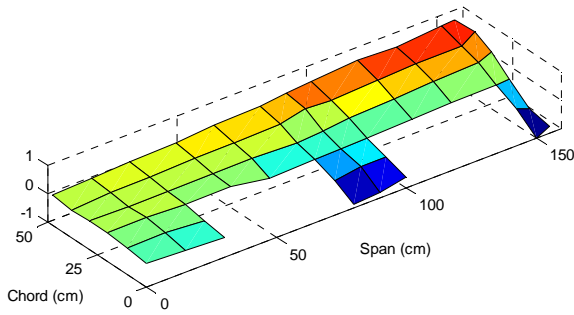


Fig. 21. Experimental 1st torsional mode shape of the mission adaptive wing ($f=49.00$ [Hz])

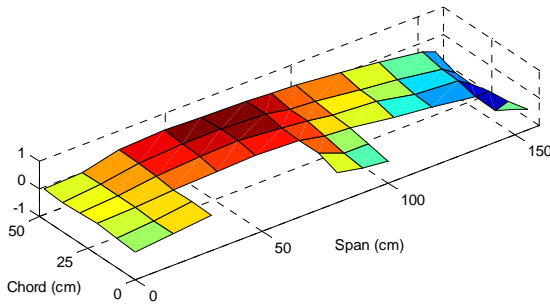


Fig. 22. Experimental 2nd out-of-plane mode shape of the mission adaptive wing ($f=88.75$ [Hz])

Comparison of the experimentally obtained resonance frequencies with the natural frequencies of the Finite Element Analysis is presented in Table II. Fig. 23 shows the final form of the unmanned aerial vehicle [9] having mission adaptive wing.



Fig. 23. Unmanned aerial vehicle with its mission adaptive wing

TABLE II
COMPARISON OF THE EXPERIMENTALLY OBTAINED RESONANCE FREQUENCIES WITH NATURAL FREQUENCIES OF THE FINITE ELEMENT ANALYSIS

Mode Shape	Experimental [Hz]	FEA [Hz]	Percentage Difference wrt Experimental
1 st Out-of-plane Bending	13.00	13.52	+ 3.84 %
1 st Torsional	49.00	46.30	- 5.83 %
2 nd Out-of-plane Bending	88.75	87.69	- 1.21 %

V. CONCLUSION

In this study the structural design, analysis and experimental modal testing of an unmanned aerial vehicle wing having mission adaptive characteristics were presented. The validation of the finite element model was performed via experimental model testing and the results presented were observed to be in close agreement.

ACKNOWLEDGMENT

This research was supported by Turkish Scientific and Technological Research Council through the project ‘TUBITAK/107M103, Aeroservoelastic Analysis of the Effects of Camber and Twist on Tactical Unmanned Aerial Vehicle Mission-Adaptive Wings’. The authors gratefully acknowledge the support given.

REFERENCES

- [1] M. I. Friswell, D. J. Inman, “Morphing concepts for UAVs”, 21st Bristol UAV Concepts Conference, April 2006.
- [2] L. Ünlüsoy, Structural Design and Analysis of a Mission Adaptive, Unmanned Aerial Vehicle Wing, M.S. Thesis, Middle East Technical University, February 2010.
- [3] MSC®/NASTRAN v2007 (2007), “Reference Manual”, MSC. Software.
- [4] E. Sakarya, “Structural Design and Evaluation of and Adaptive Camber Wing”, MSc. Thesis, Middle East Technical University, February 2010.
- [5] G. Seber, E. Sakarya, E. T. İnsuyu, M. Sahin, S. Ozgen, Y. Yaman, “Evaluation of a Camber Morphing Concept Based on Controlled Flexibility”, International Forum on Aeroelasticity and Structural Dynamics, 2009.
- [6] Product Data Sheet: Bruel&Kjaer 4508B Miniature DeltaTron Accelerometer.
- [7] Product Data Sheet: Bruel&Kjaer 4825 Modal Shaker.
- [8] Product Data Sheet: Bruel&Kjaer 8206 Impact Hammer.
- [9] E. T. İnsuyu, Aero-Structural Design and Analysis of an Unmanned Aerial Vehicle and its Mission Adaptive Wing, M.S. Thesis, Middle East Technical University, February 2010.